Proceedings of the 17th World Congress
The International Federation of Automatic Control
Seoul, Korea, July 6-11, 2008

Robust multi-objective control for the station keeping of the interferometric cartwheel

D. Arzelier * **A. Théron** * **D. Peaucelle** * **J. Fourcade** **

* *LAAS-CNRS, 7 Avenue du Colonel Roche, 31 077 Toulouse, Cedex 4, France, emails: arzelier@laas.fr, atheron@laas.fr, peaucell@laas.fr*
** *CNES, DTS/MPI/MS, BPI 1712, 18 avenue Edouard Belin, 31401 Toulouse Cedex 9, France, email: Jean.Fourcade@cnes.fr*

Abstract: Groups of satellites flying in formation require maintaining the specific relative geometry of the formation with high precision. This requirement implies to consider the problem of relative station keeping in a renewed framework. In this framework, issues related to the derivation of reliable relative models as well as to the peculiarity of the synthesis problems must be jointly considered. This paper presents some preliminary results of a robust multi-objective control approach applied to the station keeping of a low Earth observation system, i.e. the interferometric cartwheel, patented by CNES. This wheel is made up of three receiving spacecrafts, which follow an emitting Earth observation radar satellite. The particular geometry of this formation of satellites leads to the derivation of a simplified uncertain state-space model. Atmospheric drag perturbations are included in the linearized equations of the relative motion and the atmospheric density part of the definition of the atmospheric drag force is considered to be uncertain due to its dependence upon the solar activity. In the first part of the paper, an uncertain polytopic state-space model is derived. The second part describes the station keeping strategy of the formation. The station keeping strategy is performed using pure passive actuators. Due to the high stability of the relative eccentricity of the formation, only the relative semi major axis has to be controlled. Differential drag due to a differential orientation of the solar panel is used here to control relative altitude. A robust multi-objective control strategy via state-feedback is developed and tested as autonomous orbit controller. These results are analyzed via highly non linear simulations performed on a platform of CNES.

Keywords: Robust Multi-objective control, Space vehicles, Formation flight, Differential drag control

1. INTRODUCTION

Formation flight of satellites is one of the most prominent subjects of interest among space agencies and labs [1], [13], [11]. This interest is mainly due to the advantages of using numerous spacecrafts flying in a close formation rather than a single larger spacecraft. This new paradigm in space mission design would allow the reduction of mission costs as well as risks during the launching phase. Adding flexibility through reconfiguration and robustness through redundancy to space-based programs is also one of the major goal of these new developments. Moreover, enhancements in the quality of scientific instruments distributed on the formation is expected when designing a telescope with a greater focal distance and for interferometry applications for instance. D. Massonnet has proposed the idea, patented by CNES [8], of using passive Myriade microsatellites flying in a specific close formation named the interferometric cartwheel with an emitting SAR (Synthetic Aperture Radar) satellite [9]. Thanks to a specific orbital configuration defined by a slight eccentricity and adequate phasing, the formation of three satellites apparently reversely rolls along an ellipse which center follows the orbit of the reference satellite. Different possibilities have been proposed for the reference satellite: European satellites ENVISAT-L [10], TERRASAR-X [17] or Japanese satellite ALOS.

This paper presents some preliminary results of a robust multi-objective control approach applied to the station keeping of the interferometric cartwheel. In general, groups of satellites flying in formation requires maintaining the specific relative geometry of the formation with high precision. This requirement implies to consider the problem of relative station keeping in a renewed framework. In this framework, issues related to the derivation of reliable relative models as well as to the peculiarity of the synthesis problems must be jointly considered. Here, atmospheric drag perturbations are included in the linearized equations of the relative motion and the atmospheric density part of the definition of the atmospheric drag force is considered to be uncertain due to its dependence upon the solar activity. In the first part of the paper, an uncertain polytopic state-space model adapted to the specific orbital configuration of the wheel is derived. The second part describes the station keeping strategy of the formation. Two kinds of constraints are imposed by the interferometric devices : a constraint on the distance between the wheel and the radar satellite, and

constraints on the distance between the wheel satellites. The first constraint is fulfilled with a classical chemical station keeping strategy that has been defined in [4] and is not recalled here. The second one is fulfilled using pure passive actuators. Differential drag is used here to control relative altitude. The amount of surface area in the direction of satellite motion may be altered by controlling their global attitude or the differential orientation of the solar panel between two satellites of the formation. A robust multi-objective state-feedback control system is developed to modulate the drag force exerted on each satellite of the formation in response of the inter-satellite positional error. Due to the high stability of the relative eccentricity of the formation, only the relative semi major axis has to be controlled via the mean nodal elongation. These results are analyzed via highly non linear simulations performed on a platform of CNES showing the interest of this simplified approach.

2. A SIMPLIFIED DYNAMICAL MODEL OF THE INTERFEROMETRIC CARTWHEEL

The first step of the synthesis procedure consists in deriving a sufficiently simple model of the relative motion of the formation for synthesis purpose. The reference orbit in the Earth-Centered Inertial frame R_i is described via the usual orbital elements (a, e, i, Ω, ω, M) respectively defined as the semi-major axis, eccentricity, inclination, right ascension of the ascending node, argument of periapsis and mean anomaly. The orbital parameters are particularly suited to describe the geometry and the relative motion attached to the interferometric cartwheel.

2.1 The geometry of the wheel

The interferometric cartwheel is a formation made up of three receiving micro-satellites located from 30 km to 150 km behind or ahead of the reference satellite. The three satellites are located at the edges of a triangle turning on a wheel at 5 to 10 km of distance from each other (cf. figure 1). The orbit of the reference satellite is quasi-circular (eccentricity $e = 7.1355\ 10^{-5}$) and defined by its semi-major axis a of orbital period T.

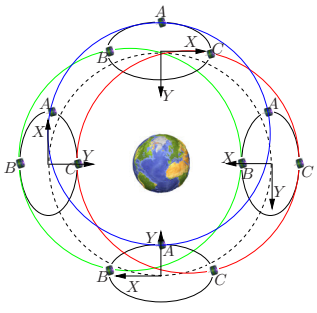

Fig. 1. Motion of the wheel during an orbital period

The orbits of the receiving satellites A, B, C have the same major-axis but with a slight modification in the eccentricity ($e_i = e + \Delta e,\ i = A, B, C$). The relative motion of the three satellites with respect to the reference orbit is an ellipse defined in the reference orbital plane. The semi-major axis of this ellipse is given by $2a\Delta e$ while the semi-minor axis is $a\Delta e$ (cf. figure 2).

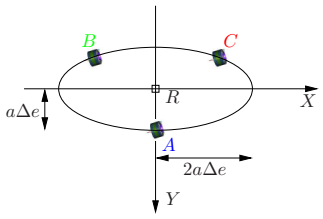

Fig. 2. Geometry of the interferometric cartwheel

When building a wheel composed of three satellites with an identical extra eccentricity, arguments of perigee ω_i of receiving satellites must be equally distributed every 120 deg. along the orbit (cf. figure 3). As will be seen in the sequel, the particular geometry of this formation of satellites leads to the derivation of a simplified uncertain state-space model.

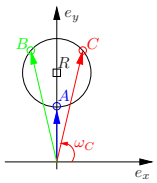

Fig. 3. Eccentricty vectors for the receiving satellites

Considering that each receiving satellite roll along its own wheel, the problem of station keeping of a unique wheel for the three satellites amounts to respect the following requirements.

- Orbital planes of the individual wheels are identical.
- The centers of the individual wheels follows the same quasi-circular orbit i.e. all semi-major axis of individual wheels are identical to the semi-major axis of the reference orbit.
- The eccentricities of each individual wheel are identical.
- The mean argument of latitude $\alpha_i = \omega_i + M_i$ must be the same for all receiving satellites.

As in the reference [4], the problem of station keeping of the wheel mainly consists in controlling the relative positions of the centers of the individual wheels all along the orbit. The center of the wheel is principally characterized by the mean argument of latitude $\alpha = \omega + M$. It is therefore assumed that eccentricity is not affected by the different orbital perturbations. The simplified station keeping strategy of the wheel proposed in this paper amounts to control the relative deviations $\delta\alpha_i$, $i = A, B, C$ against the perturbation induced by the atmospheric drag differential force. The next subsection is dedicated to the derivation of the state-space model utilized for the synthesis of a multi-objective control law.

2.2 Linearized differential equations of relative motion

A convenient frame used in orbital mechanics when atmospheric drag perturbation is considered is defined by the rotating frame $\mathcal{R} = \{\vec{t}, \vec{n}, \vec{w}\}$ where $\vec{t}$ is along the orbit velocity vector, $\vec{w}$ is normal to the orbit plane and $\vec{n}$ is chosen to complete the right-hand set of orthogonal coordinate frame unit vectors. The relative dynamics between

two satellites of the wheel used in this paper are based on a particular form of Gauss's Variational Equations (GVEs) including the atmospheric drag perturbation. In addition to the advantages detailed in [12], the use of orbital element differences is more convenient for the interferometric cartwheel description than the typical cartesian coordinate (Clohessy-Wiltshire) frame. Remember that the only orbital perturbation considered in the synthesis model is due to the atmospheric drag. The acceleration due to the atmospheric drag is classically given by:

$$\overrightarrow{\gamma}_f = \gamma_t \overrightarrow{t} = -\frac{\rho S C_D v^2}{2 m_{sat}} \overrightarrow{t} = \frac{B_\rho v^2 S}{2} \overrightarrow{t} \tag{1}$$

where S is the satellite cross-sectional area along the velocity vector, C_D is the drag coefficient, ρ is the local atmospheric density, m_{sat} is the mass of the satellite and v is the inertial velocity of the spacecraft. As the considered orbits are quasi-circular orbits and the associated eccentricity is quite small, it is necessary to introduce the eccentricity vector $[e_x \quad e_y]'$ and to define a nonsingular set of modified orbital parameters. Considering that the atmospheric drag does not introduce any perturbation on the inclination i and the right ascension of the ascending node Ω, we get the following set of modified GVEs.

$$\frac{da}{dt} = S B_\rho \sqrt{\mu \cdot a} \left[\frac{1 + 2e\cos\nu + e^2}{1 - e^2} \right]^{3/2} \tag{2a}$$

$$\frac{de_x}{dt} = S B_\rho (e_x + \cos\alpha_\nu) \sqrt{\frac{\mu(1 + 2e\cos\nu + e^2)}{a(1 - e^2)}} \tag{2e_x}$$

$$\frac{de_y}{dt} = S B_\rho \, (e_y + \sin\alpha_\nu) \sqrt{\frac{\mu(1 + 2e\cos\nu + e^2)}{a(1 - e^2)}} \tag{2e_y}$$

$$\frac{d\alpha}{dt} = S B_\rho \frac{\sin\nu}{e} \left(1 - \sqrt{1 - e^2} \left(1 + \frac{e^2}{1 + e\cos\nu} \right) \right) \times \sqrt{\frac{\mu(1 + 2e\cos\nu + e^2)}{a(1 - e^2)}} + \sqrt{\frac{\mu}{a^3}} \tag{2\alpha}$$

(2)

where $\alpha_\nu = \nu + \omega$ and ν is the true anomaly. The surface area adjustments are made by changing the attitude of the solar panel of the satellite. This type of passive actuation for the orbit control of a satellite has already been considered in [7], [6]. Let S_b and S_p be respectively the surface area of the body and of the solar panel of the satellite. φ is the angle between the panel and the velocity vector (cf. figure 4). Denoting the global surface area of the reference satellite as $S_r = S_b + S_p\varphi$, the control signal is defined by $\delta S = S_p \delta\varphi$. $\delta\varphi = \varphi_i - \varphi_r$ where $\varphi_r = 15$ deg $= \dfrac{\pi}{12}$ rad. is the angle of the solar panel of the reference satellite. Note that the variations of attitude of the solar panel has to fulfill the constraints $-\dfrac{\pi}{12} \leq \delta\varphi \leq \dfrac{\pi}{12}$. It is recalled that the control objective is

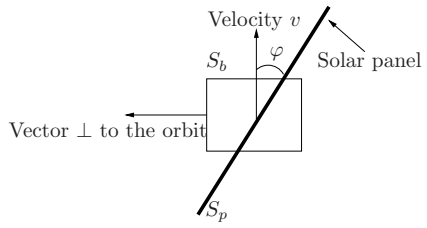

Fig. 4. Solar panel attitude

to control the relative semi-major axis δa and the relative mean argument of latitude $\delta\alpha$ between two satellites of the wheel by assuming the relative eccentricity is not drifting. It is also assumed that the rate of change of the relative semi-major axis is constant. This amounts to only consider secular drift induced by orbital perturbations.

$$\delta a = \delta a_0 + \dot{\delta a}\, t \tag{3}$$

A linearization of the GVEs (2) with respect to $e \simeq 0$ coupled with the computation of the first variations.

$$\begin{aligned} \frac{d\,\delta a}{dt} &= \frac{\partial \dot{a}}{\partial a}\delta a + \frac{\partial \dot{a}}{\partial \alpha}\delta\alpha + \frac{\partial \dot{a}}{\partial S}\delta S \\ \frac{d\,\delta\alpha}{dt} &= \frac{\partial \dot{\alpha}}{\partial a}\delta a + \frac{\partial \dot{\alpha}}{\partial \alpha}\delta\alpha + \frac{\partial \dot{\alpha}}{\partial S}\delta S \end{aligned} \tag{4}$$

lead to the derivation of the simplified state-space model for the relative motion of the wheel submitted to atmospheric drag.

$$\begin{bmatrix} \dfrac{d\,\delta\alpha}{dt} \\ \dfrac{d^2\,\delta\alpha}{dt^2} \end{bmatrix} = \begin{bmatrix} 0 & 1 \\ 0 & 0 \end{bmatrix} \begin{bmatrix} \delta\alpha \\ \dfrac{d\,\delta\alpha}{dt} \end{bmatrix} + \begin{bmatrix} 0 \\ -\dfrac{3\mu}{2a^2} B_\rho \, S_p \end{bmatrix} \delta\varphi \tag{5}$$

The dynamic model (5) is a double integrator for which the input matrix B is supposed to be uncertain due to the variation of the coefficient B_ρ as will be seen in the sequel.

2.3 Linear polytopic continuous-time state-space model

The parameter B_ρ depends upon the density ρ of the upper atmosphere for which highly sophisticated models exist in the literature. ρ is obviously related to the composition of the upper atmosphere but is also greatly affected by the incident solar flux (the incident radiation coming from the sun). It affects the atmospheric density through heating from Extreme Ultraviolet Radiation (F_{EUV}) that heats the upper atmosphere. One Solar Flux Unit (SFU) is defined as 1 SFU $= 1 \times 10^{-22} \frac{\text{watt}}{\text{m}^2\text{Hz}}$. The figure 5 depicts the time evolution of the semi-major axis for a constant solar activity $F_{EUV} = 100$ SFU.

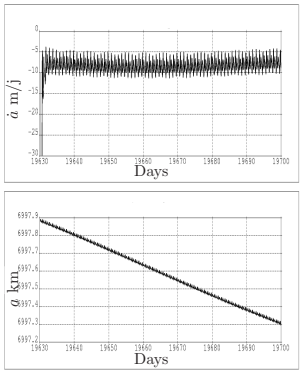

Fig. 5. a and $\dot{a}$ for a constant solar activity (100 SFU)

It can be shown that this evolution may be approximated by the following equation.

$$\dot{a} = B_\rho v^2 (S_b + S_p\phi) \sqrt{\frac{a^3}{\mu}} \tag{6}$$

Identifying $\dot{a}$ for typical values of the constant solar flux ($F_{EUV} = 100$ and $F_{EUV} = 200$) allows to deduce extreme

values for the parameter B_ρ reflecting the variability of the density due to a variable solar activity. Finally, we end up with a very simple linear polytopic model that is reminiscent to the modelling used in the reference [5].

$$\dot{x}(t) = \begin{bmatrix} 0 & 1 \\ 0 & 0 \end{bmatrix} x(t) + \begin{bmatrix} 0 \\ b \end{bmatrix} u(t) \tag{7}$$

where $b \in [\underline{b}\ ,\ \overline{b}]$ with $b = -\frac{3\mu}{a^2} B_\rho S_p$ and $0 < \underline{b}$. The next section is dedicated to the synthesis of a robust multi-objective state-feedback controller for the polytopic model (7).

3. AN ANALYTICAL SOLUTION FOR THE ROBUST MULTI-OBJECTIVE CONTROL OF THE POLYTOPIC DOUBLE INTEGRATOR

The main control objectives are first, to realize the absolute station keeping of the wheel behind the emitting radar satellite and second, to maintain the relative geometry of the cartwheel. As mentioned in the introduction, it is assumed in this paper that the first goal is achieved thanks to a classical chemical station keeping strategy exposed in [15]. The second set of maneuvers is aimed at controlling the relative mean nodal elongation $\delta\alpha$ between each couple of satellites of the wheel in a range of $\pm$ 0.004 deg or a margin of 500 m [15] of distance in face of various orbital perturbations. Here below is developed a multi-objective control strategy based on a robust state-feedback pole placement of the closed-loop relative dynamics of the model (7) in some specific region of the complex plane. A set of state-feedback controllers fulfilling the robust pole placement requirement is graphically sketched out and the robust H_2 optimal state-feedback law is analytically identified.

3.1 Robust pole placement via state-feedback

The first requirement imposed on the closed-loop relative dynamics is that time responses must be be sufficiently damped and fast without saturating the actuators which maximal value is limited to $\pm\ \frac{\pi}{12}$. It is therefore required that the closed loop poles of the model (7), when applying a state-feedback control law, must be robustly located in the region depicted at figure 6 for all variation of the parameter $b \in [\underline{b}\ ,\ \overline{b}]$. This region, as the intersection of three LMI regions [2], is an LMI region composed of a half-plane, a disk and a sector. It is characterized by three parameters α_1, r, ξ and is denoted $\mathcal{D}(\alpha_1, r, \xi)$. Writing down the conditions for the poles of the closed-loop uncertain dynamical matrix $A = \begin{bmatrix} 0 & 1 \\ bK_1 & bK_2 \end{bmatrix}$ to belong to $\mathcal{D}(\alpha_1, r, \xi)$ leads to the following constraints on the entries K_1 and K_2 of the state-feedback controller.

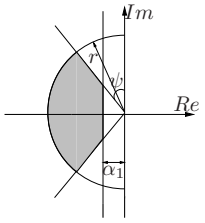

Fig. 6. $\mathcal{D}(\alpha_1, r, \xi)$ LMI region for robust pole placement

- Damping condition and disk condition for complex poles:

$$\frac{2\xi}{\sqrt{\underline{b}}} \leq \frac{-K_2}{\sqrt{-K_1}} \quad , \quad -K_1 < \frac{r^2}{\overline{b}} \tag{8}$$

- Relative stability condition:

$$\begin{array}{l} \dfrac{2\alpha_1}{\underline{b}} \geq K_2 \quad , \quad K_2 > \dfrac{-K_1}{\alpha_1} + \dfrac{\alpha_1}{\overline{b}} \\ \dfrac{2\alpha_1}{\underline{b}} \geq K_2 \quad , \quad \dfrac{2}{\sqrt{\overline{b}}} < \dfrac{-K_2}{\sqrt{-K_1}} \end{array} \tag{9}$$

- Disk condition:

$$K_2 > \frac{K_1}{r} - \frac{r}{\overline{b}} \quad , \quad \frac{-2r}{\overline{b}} < K_2 \quad , \quad \frac{2}{\sqrt{\overline{b}}} < \frac{-K_2}{\sqrt{-K_1}} \tag{10}$$

These conditions allow to plot the non convex bounded set of realizable gains $\mathcal{K}_\mathcal{D}$ in the (K_1, K_2) plane for a given region $\mathcal{D}(\alpha_1, r, \xi)$ (see figure 7). This set may be empty if the parameters α_1, r, ξ define a too stringent region depending upon the range of variations of the uncertain parameter b. It is then possible to give explicit constraints on α_1, ξ and r.

$$\frac{\overline{b}}{\underline{b}} < \frac{-r}{\alpha_1} \quad , \quad \frac{2r\alpha_1}{\underline{b}} + \frac{r^2}{\overline{b}} > -\frac{\alpha^2}{\underline{b}\xi^2} \tag{11}$$

For a standard choice of $\xi = \sqrt{2}2$, conditions (11) imply to have a ratio $\frac{r}{\alpha_1}$ of about 20. This mixed graphical/analytical method is possible because of the simplicity of our model. In case of more complex uncertain dynamics, a Lyapunov approach may be used instead [2].

3.2 Analytical solution for the multi-objective control problem

In order to limit the activity of the actuators as well as the transient oscillations energy of the mean nodal elongation time response, an H_2 performance criterion is defined on the following standard model [14]:

$$\begin{array}{l} \dot{x} = \begin{bmatrix} 0 & 1 \\ 0 & 0 \end{bmatrix} x + \begin{bmatrix} 0 \\ b \end{bmatrix} u + \begin{bmatrix} 0 \\ 1 \end{bmatrix} w = Ax + B_u u + B_w w \\ z = \begin{bmatrix} 1 & 0 \\ 0 & 0 \end{bmatrix} x + \begin{bmatrix} 0 \\ 1 \end{bmatrix} u = C_z x + D_{zu} u \\ u(t) = Kx(t) \end{array} \tag{12}$$

where w is a perturbation and z the controlled output. Denoting the closed-loop transfer from z to w by $T_{zw}(K, b)$, the robust multi-objective control problem to solve is defined by the following min-max problem:

$$\min_{K \in \mathcal{K}_\mathcal{D}} \max_{b \in [\underline{b}\ ,\ \overline{b}]} \|T_{zw}(K, b)\|_2 \tag{13}$$

Using the standard definition of the H_2 norm of a system in terms of the controllability grammian, the previous problem may be recast as the following.

$$\begin{array}{lll} \min\limits_{\substack{K \in \mathcal{K}_\mathcal{D} \\ P \in \mathcal{S}_n^+}} & \max\limits_{b \in [\underline{b}\ ,\ \overline{b}]} & \mathrm{Trace}[C_z(K) P C_z'(K)] \\ \text{under} & & A(K,b)P + PA'(K,b) + B_w B_w' = \mathbf{0} \end{array} \tag{14}$$

where $C_z(K) = \begin{bmatrix} 1 & 0 \\ K_1 & K_2 \end{bmatrix}$. After some elementary developments, we end up with the parametric optimization problem:

$$\min_{K \in \mathcal{K}_\mathcal{D}} g(K_1, K_2) = \frac{1 + K_1^2 - K_2^2 K_1 \underline{b}}{2\underline{b}^2 K_1 K_2} \tag{15}$$

Plotting the level set of the function $g(K_1, K_2)$ over the realizability region $\mathcal{K}_\mathcal{D}$ leads to the identification of the optimal pair (K_1^*, K_2^*) and of the worst-case H_2 norm of T_{zw}.

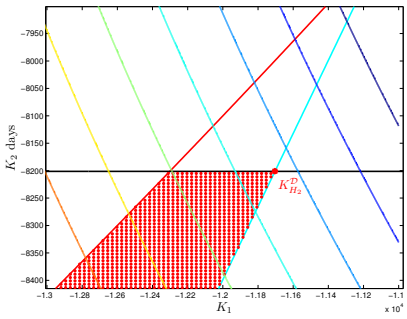

Fig. 7. Region of realizability in the (K_1, K_2) plane and robust optimal solution for $\mathcal{D}(-1.5, 35, \frac{\sqrt{2}}{2})$

$$\begin{aligned} K_{H_2}^{\mathcal{D}} &= \left[-\alpha_1^2 \left(\frac{-2}{\underline{b}} + \frac{1}{\underline{b}}\right) \frac{2\alpha_1}{\underline{b}} \text{ days} \right] = \left[K_1^* \;\; K_2^* \right] \\ \|T_{zw}(K_{H_2}^{\mathcal{D}}, \underline{b})\|_2 &= \sqrt{\frac{1 + K_1^{*2} - K_2^{*2} K_1^* \underline{b}}{2\underline{b}^2 K_1^* K_2^*}} \end{aligned} \tag{16}$$

These results are now simulated on a professional platform of simulation developed by the CNES, named PSIMU© and using a set of realistic data.

4. SIMULATION RESULTS

For the synthesis of the multi-objective control law, the range of variations for b is given by the identification of extreme solar activity for respectively a solar flux of 100 and 200 leading to $b \in [0.0003658 \; ; \; 0.0038]$. It is therefore possible to design a multi-objective controller that robustly places the closed-loop poles in the region $\mathcal{D}(-1.5, 35, \frac{\sqrt{2}}{2})$ and minimizes the H_2 norm of the transfer $T_{zw}(K, b)$ in the worst-case.

$$\begin{aligned} K_{H_2}^{\mathcal{D}} &= [\, -11704 \;\; -8202 \text{ days} \,] \\ \|T_{zw}(K_{H_2}^{\mathcal{D}}, \underline{b})\|_2 &= 4067.3 \end{aligned} \tag{17}$$

In order to analyze this last control law, the orbital parameters are defined in table 1 for the specification of the geometry of the wheel. Note that the difference of the initial ν is equivalent to a difference of mean nodal elongation of $a_\times \delta\nu = 45$ m and that no measurement noise has been considered in the following simulations. The figures 8 and 9

	Leader	Follower
a	7007137 m	7007137 m
e	$7,1355\ 10^{-5}$	$7,1355\ 10^{-5}$
Ω	0	0
i	97 deg	97 deg
ω	0	0
ν	0	$6,4220\ 10^{-6}$ rad

Table 1. Orbital parameters

give the time response of the relative $\delta\phi$, $a \times \delta\alpha$ and relative semi-major axis for a constant solar activity including a very complete set of orbital perturbations (atmospheric drag, solar radiation pressure, sun and moon perturbing accelerations, zonal and tesseral of order 10 gravitational perturbations). The station keeping objectives appear to be satisfied in terms of precision since we get 8 10^{-5} deg. for the mean nodal elongation. A simulation, not presented here for conciseness reasons, performed on a longer horizon (360 days) shows that the apparent drifting at the end of the simulations presented here corresponds to a long-term (300 days) oscillation of 30 m (2.4 10^{-4} deg.) amplitude for the mean nodal elongation. This periodic perturbation may come from the fact that zonal harmonic perturbations (J_2 for instance) have not been considered in the design of the control law.

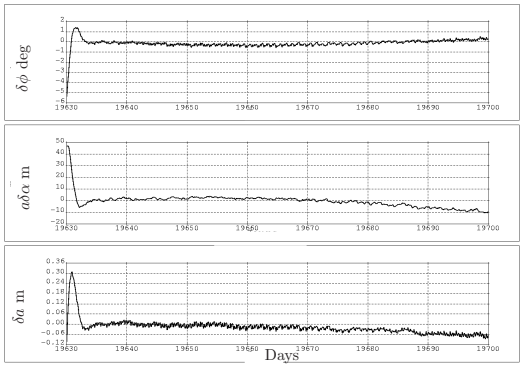

Fig. 8. Constant solar activity $F_{EUV} = 100$ SFU

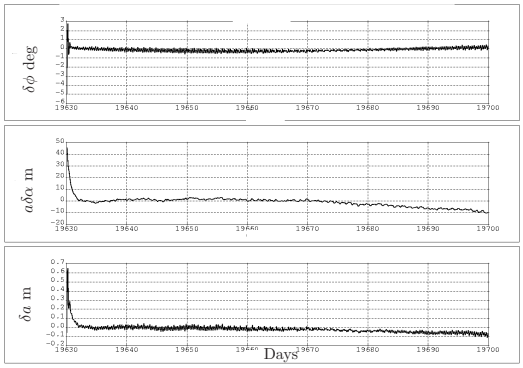

Fig. 9. Constant solar activity $F_{EUV} = 200$ SFU

Finally, a simulation of the control law is performed by considering a real solar activity depicted in figure 10. This activity has been measured during 70 days from October 1983 and shows extreme values of solar flux ranging from 90 SFU to 300 SFU.

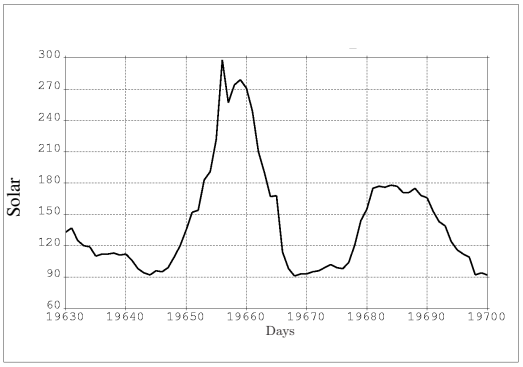

Fig. 10. Solar activity in October 1983

The time responses of figure 11 clearly demonstrates the capacity of the control law to reject high level perturbations. The obtained precision of the station keeping appears to be satisfactory.

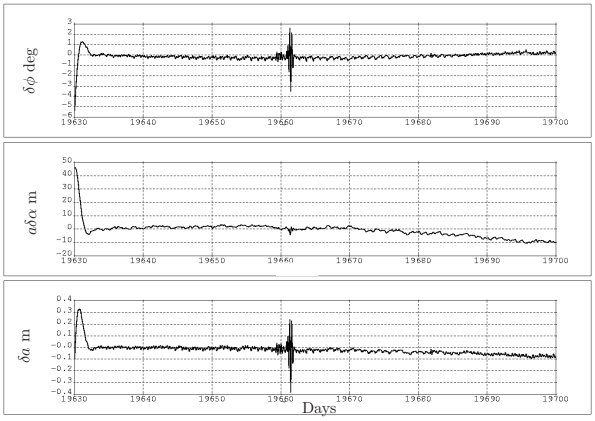

Fig. 11. Time evolution for a real solar activity

5. CONCLUSION

A very simple model (double integrator for the dynamic of the relative mean nodal elongation) of the relative motion of the interferometric cartwheel has been used for the design of a robust station keeping control law via passive actuation and differential drag control. These preliminary results appear to be really promising when compared to the ones presented in [5]. We believe that this first paper may pave the way for more involved studies in the future. More complex uncertain models for the relative motion of the wheel (including semi-major axis and eccentricity dynamics) should be elaborated. Additional orbital perturbations have to be taken into account to get more insensitive control laws with respect to periodic perturbations effects. Another way to tackle this last issue could be to consider mean orbital parameters leading therefore to the synthesis of a sampled-data control system.

REFERENCES

[1] K.T. Alfriend, H. Schaub, "Dynamics and control of spacecraft formations: Challenges and some solutions", *Journal of the Astronautical Sciences*, Vol. 48, No. 2, pp. 249-267, 2000.

[2] D. Arzelier, D. Henrion, D. Peaucelle, "Robust $\mathcal{D}$ stabilization of a polytope of matrices", *International Journal of Control*, Vol. 75, No. 10, pp. 744-752, 2002.

[3] L. Breger, J.P. How, "Gauss's variational equation-based dynamics and control for formation flying spacecraft", *Journal of Guidance, Control and Dynamics*, Vol. 30, No. 2, pp. 437-448, 2007.

[4] J. Fourcade, "TerraSAR-L Interferometric Cartwheel", *Technical report ESA RIRTL-NT-0-5-CNES*, November 2003.

[5] J. Fourcade, "Mission Analysis and Orbit Control of Interferometric Wheel Formation Flying", *ESA Special Publication*, Vol. 548, 2004.

[6] J. Franconeri, "Use of differential Drag as a Satellite Constellation Station Keeping Strategy", *ASEN 5050, http://ccar.colorado.edu/asen5050/projects/*, December 2003.

[7] C.L. Leonard, W.M. Hollister, E.V. Bergmann, "Orbital formationkeeping with differential drag", *Journal of Guidance*, Vol. 12, No. 1, pp. 108-113, 1989.

[8] D. Massonnet, "Roue Interfromtrique", *French Patent 236910D17306RS*, April 1998.

[9] D. Massonnet, "Capabilities and limitations of the interferometric cartwheel", *IEEE Transactions on Geoscience and Remote Sensing*, Vol. 39, No. 3, pp. 506-520, 2001.

[10] H.R. Runge, J. Mittermayer, F. Jochim, D. Massonnet, E. Thouvenot, "The interferometric cartwheel for Envisat", *Proceedings of the 3rd IAA Symposium on Small Satellites for Earth Observation*, Berlin, Germany, April 2001.

[11] D.P. Scharf, F. Hadaegh, S.R. Polen, "A survey of spacecraft formation flying guidance and control (part II): Control", *American Control Conference*, Boston, Massachusetts, USA, pp. 2976-2985, July 2004.

[12] H.H. Schaub, J.L. Junkins, *Analytical mechanics of space systems*, AIAA Editions, Education Series, Reston, Virginia, USA, 2003.

[13] M. Tillerson, G. Inalhan, J.P. How, "Co-ordination and control of distributed spacecraft systems using convex optimization techniques", *International Journal of Robust and Nonlinear Control*, Vol. 12, No. 2-3, pp. 207-242, 2002.

[14] K. Zhou, J.C. Doyle, K. Glover, *Robust and Opimal Control*, Prentice Hall, Englewood Cliffs, New Jersey, 1996.

[15] A. Vacaresse, P. Brousse, "Interferometric wheel orbit control", *Proceedings of the International Symposium on Spaceflight Dynamics*, Biarritz, France, 2000.

[16] S.R. Vadali, S.S. Vaddi, K. Naik, K.T. Alfriend, "Control of satellite formation", *AIAA paper 2001-4028*, August 2001.

[17] M. Zink, G. Krieger, N. Amiot, "Interferometric performance of a cartwheel constellation for TerraSAR-L", *Proceedings of the ESA Fringe Workshop*, Frascati, Italy, 2003.